Optically Active Covalent Organic Frameworks and Hyperbranched Polymers with Chirality Induced by Circularly Polarized Light

SCHOLARONE™
Manuscripts

COMMUNICATION

Optically Active Covalent Organic Frameworks and Hyperbranched Polymers with Chirality Induced by Circularly Polarized Light

Yuting Wang,[a] Koji Yazawa,[b] Qingyu Wang,[a] Takunori Harada,[c] Shuhei Shimoda,[d] Zhiyi Song,[a] Masayoshi Bando,[a] Naofumi Naga,[e] and Tamaki Nakano [*a,f]

Axial chirality was induced by circularly polarized light to covalent organic frameworks as well as hyperbranched polymers composed of bezene-1,3,5-triyl core units and oligo(benzene-1,4-diyl) as linker units where variation in induction efficiency was rationally interpreted in terms of internal rotation dynamics studied through CPMAS ^{13}C NMR experiments including CODEX measurements.

Chiral polymers are an important class of materials because of their wide scope of applications.[1,2] While most studies have targeted linear polymers with a single-handed helical conformation controlled by chiral monomeric units or by catalysis or by external stimuli, chiral dendrimers and hyperbranched polymers (HBP's) composed of chiral units have also been reported.[3-5] In addition, as newer chiral polymers with branching, covalent organic frameworks (COF's) has been drawing attention.[6-8] Chiroptical properties of COF's arise mostly from chiral constituent units except in one exception where an optically active small molecule induced chirality through non-covalent interactions.[8] With such a background, we herein report the preparation of optically active COF's and HBP's composed of benzene-1,3,5-triyl core and oligo(benzene-1,4-diyl) linker units having preferred-handed axial chirality (twist) around benzene-benzene junctions induced by circularly polarized light (CPL). Preparation of optically active COF's and HBP's based on chirality of light has been unprecedented.

Chirality induction by CPL has been realized for linear polyfluorene derivatives and other small molecules having aromatic-aromatic (Ar-Ar) single bonds through enantiomer-selective excitation of axially chiral Ar-Ar units.[9-13] Biphenyl as the simplest Ar-Ar compound has a twisted conformation in the ground state and is transformed to a coplanar conformation in excited states (twisted-coplanar transition),[14,15] and if one of the enantiomeric twists is preferentially excited by CPL, the population of the un-excited twist increases, which leads to an optically active product (twist-sense-selective excitation).[9-13,16-18] In this work, this methodology was applied for the COF's and HBP's composed of benzene-benzene junctions. CPL-based chirality induction has been reported also for polymers having azobenzene moieties as part of constitutional uints[19-23] and for solid-state polymerization systems[24] as well as for small-molecular systems.[25,26]
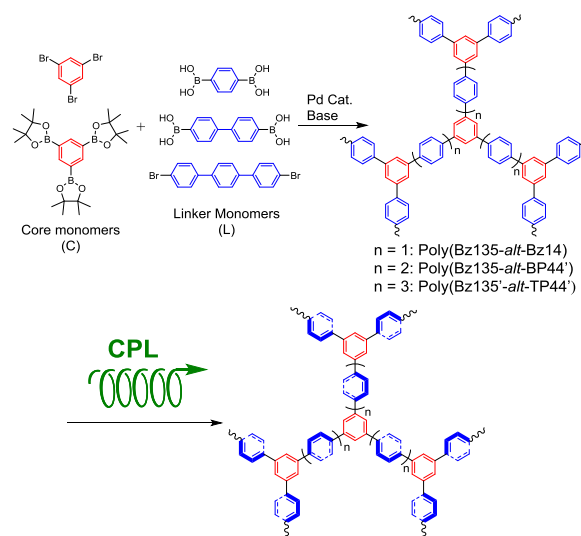
Scheme 1. Synthesis of COF's and HBP's composed of benzene rings and chirality induction them by CPL.

Suzuki-Miyaura cross coupling reactions of core monomer (C) with a linker monomer (L), namely, the reactions of 1,3,5-tribromobenzene with 1,4-bis(dihydroxyboranyl)benzene,   1,3,5-tribromobenzene with 4,4,'-bis(dihydoxyboranyl)-1,1'-biphenyl,   and   1,3,5-tris(4,4,5,5-tetramethyl-1,3,2-dioxaborolan-2-yl)benzene   with   4,4''-dibromo-1,1':4',1''-terphenyl led to poly(benzene-1,3,5-triyl-*alt*-benzene-1,4-diyl) [poly(Bz135-*alt*-Bz14)],   poly(benzene-1,3,5-triyl-*alt*-1,1'-biphenyl-4,4'-diyl) [poly(Bz135-*alt*-BP44')], and poly(benzene-1,3,5-triyl-*alt*- 1,1':4',1''-

[a.] Institute for Catalysis (ICAT) and Graduate School of Chemical Sciences and Engineering, Hokkaido University, N21W10, Kita-ku, Sapporo 001-0021, Japan E-mail: tamaki.nakano@cat.hokudai.ac.jp.
[b.] JEOL RESONANCE Inc., 3-1-2 Musashino, Akishima, Tokyo 196-8558, Japan
[c.] Department of Integrated Science and Technology, Faculty of Science and Technology, Oita University, Dannoharu, 700, Oita City 870-1192, Japan
[d.] Technical Division, Institute for Catalysis, Hokkaido University, N21W10, Kita-ku, Sapporo 001-0021, Japan
[e.] Department of Applied Chemistry, Shibaura Institute of Technology, College of Engineering, 3-7-5 Toyosu, Koto-ku, Tokyo 135-8548, Japan
[f.] Integrated Research Consortium on Chemical Sciences (IRCCS), ICAT, Hokkaido University, Sapporo 001-0021, Japan
Electronic Supplementary Information (ESI) available: [details of any supplementary information available should be included here]. See

terphenyl-4,4''-diyl) [poly(Bz135-*alt*-TP44'')], respectively, at different [L]/[C] ratios (Scheme 1).[27-29]

The polymerization products were composed of tetrahydrofuran-(THF)-soluble part having a network structure (COF) and THF-soluble part having no cross linking (HBP) (Tables S1-S3 in ESI). The apparent averaged molar masses of the HBP's were less than about 1×10^3 (SEC, vs. polystyrene) while selected samples indicated mean diameters of ca. 16-80 nm in dynamic light scattering measurements (Fig. S14 in ESI), suggesting that true molar masses may be much higher than the SEC-based values.

The three COF's were irradiated with CPL in fine powder form sandwiched between two quartz plates. Upon irradiation, poly(Bz135-*alt*-TP44'') COF exhibited, intense and clear CD spectra, and the spectra obtained on L- and R-CPL irradiation were almost mirror images (Fig. 1 A and Fig. S16 in ESI), indicating that preferred-handed twist conformation was induced to benzene-benzene junctions through twist-sense-selective excitation. The chemical structure of the COF was found intact through CPL irradiation by IR spectra (Fig. S10 in ESI). In addition, the induced chirality was stable over months at ambient temperature.

LD spectral measurements supported that the CD spectra in Fig. 1A arise from material chirality and not from film anisotropy (Figure S27 in ESI).
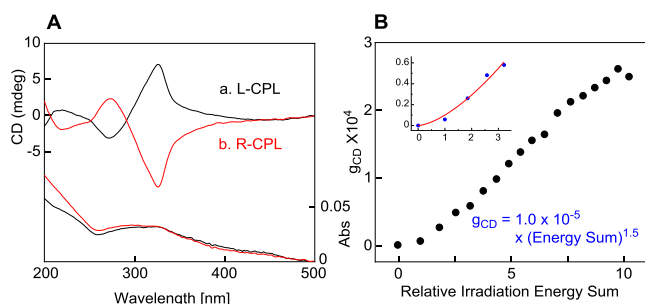

Fig. 1. CD-UV spectra of poly(Bz135-*alt*-TP44'') COF (run 3 in Table S3-2 in ESI) observed on L-CPL (a) and R-CPL (b) irradiation [A] and g_{CD}-vs.-relative irradiation energy sum plots with curve fitting results (inset plots and corresponding equation) [B]. Maximum g_{CD} was $+2.5 \times 10^{-4}$ at 326 nm.

The evolution in g_{CD} spectra was accompanied with a decrease in absorbance spectral intensity (Figs. S18 and S19 in ESI). This observation is ascribed to a change in the average dihedral angle around single bonds which has been clarified for biphenyl molecule by combined theoretical and experimental studies.[30]

CD intensity is discussed in terms of the Kuhn's anisotropy factor [$g_{CD} = 2(\varepsilon_L - \varepsilon_R)/(\varepsilon_R + \varepsilon_L)$ where ε_L and ε_R are molar absorptivities toward left-handed and right-handed CPL's, respectively][31] to eliminate the influence of absorbance intensity. Fig. 1 B shows the plots of g_{CD} observed on L-CPL irradiation against relative irradiation energy sum at 326 nm whose definition is found in ESI. The g_{CD}-vs.-energy sum plot does not show a first-order type relation (an increasing form of exponential decay), and the early-stage data can be well approximated with the power function indicated within Fig. 1 B. Further, the maximum g_{CD} of $+2.5 \times 10^{-4}$ at 326 nm after saturation of CD intensity upon L-CPL irradiation was much higher than expected for aromatic compounds on the basis solely of CPL chirality. Aromatic compounds at 100% e.e. generally show g_{CD} values of 10^{-3} to 10^{-4} order,[16,32] and g_{CD}

values attainable based only on CPL without amplification are of 10^{-6} to 10^{-8} order because the maximum e.e. values (γ_{PSS}) attainable at photo stationary state follows the equation, $\gamma_{PSS} = 1/2 \, g_{CD(100\% \, e.e.)} \times 100 \%$, which leads to maximum g_{CD} values decided by the equation, $g_{CD} = 1/100 \times \gamma_{PSS} \times g_{CD(100\% e.e.)} = 1/2(g_{CD(100\% e.e.)})^2$.[16,33] These results suggest that efficient chirality amplification took place through CPL irradiation to the COF.

On the other hand, poly(Bz135-*alt*-BP44') COF showed much weaker CD spectra, and poly(Bz135-*alt*-Bz14) COF did not respond to CPL irradiation (Fig. S16 in ESI). Regarding the differences among the three COF's, the three COF's showed rather similar transmission electron microscopy (TEM) images without any particularly regular structures (Fig. 2 top) while poly(Bz135-*alt*-Bz14) COF showed clear electron diffraction (ED) spots and the other two COF's did not (Fig. 2 bottom). On the other hand, none of the three COF's showed any diffraction patterns indicating molecular ordering in XRD measurements (Fig. S15 in ESI). These results may mean that poly(Bz135-*alt*-Bz14) COF has a short-distance ordered packing of benzene rings detected by ED but not by XRD. CPL irradiation may not induce effective rotation for poly(Bz135-*alt*-Bz14) COF due to a rigid structural order.
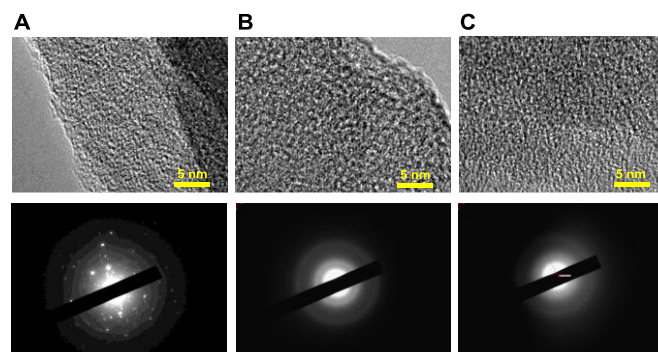

Fig. 2. TEM images (top) and electron diffraction profiles (bottom) of poly(Bz135-*alt*-Bz14) COF (run 4 in Table S1 in ESI) (A), poly(Bz135-*alt*-BP44') COF (run 3 in Table S2 in ESI) (B), and poly(Bz135-*alt*-TP44'') COF (run 3 in Table S3-2 in ESI) (C).].

Further, solid-state NMR analyses were conducted to probe the twisting motion in the COF's. The ^{13}C CPMAS spectra of COF's (Fig. 3 A) showed two main signals of benzene rings corresponding to "C4" having no hydrogens and to "C3" having hydrogens at around 140 ppm and 127 ppm, respectively. The three spectra showed slightly different patterns which may reflect the difference in chemical structure among the three COF's.

To investigate the twisting motion, we first carried out ^{13}C longitudinal relaxation time at rotating flame ($T_{1\rho C}$) measurements which is sensitive to kHz order molecular motion. Three COF's indicated clear dependence of $T_{1\rho C}$ on the structure (Fig. S6 in ESI). The decay profiles of C3 signals were well fitted with double exponential functions leading to shorter and longer relaxation times ($T_{1\rho C}^{fast}$, $T_{1\rho C}^{slow}$) while those of C4 signals with single exponential functions leading to one relaxation time ($T_{1\rho C}$) (Figs. S7-S9 in ESI). Considering the C3 signals arise from the carbons at the 2- and 3-positions of the bezene-1,4-diyl "linker" units and those at the 2-, 4-, and 6-positions of the benzene-1,3,5-triyl "core" units, $T_{1\rho C}^{fast}$ and $T_{1\rho C}^{slow}$ probably reflect molecular motions of the former and the latter, respectively. The most plausible motion contributing to $T_{1\rho C}^{fast}$ is twisting (flipping) of the bezene-1,4-diyl units around the chirality axes,

and it was shorter for poly(Bz135-*alt*-TP44'') COF (1.9 ms) than for the other two COF's showing similar values (3.4 ms, 3.0 ms), indicating that the small-angle twisting motion is faster for the former COF than the other two. $T_{1\rho C}^{slow}$ of C3 and $T_{1\rho C}$ of C4 may reflect motions of the relevant carbons other than rotation including changes in their relative orientation within the COF structures which could occur in association with the rotation.
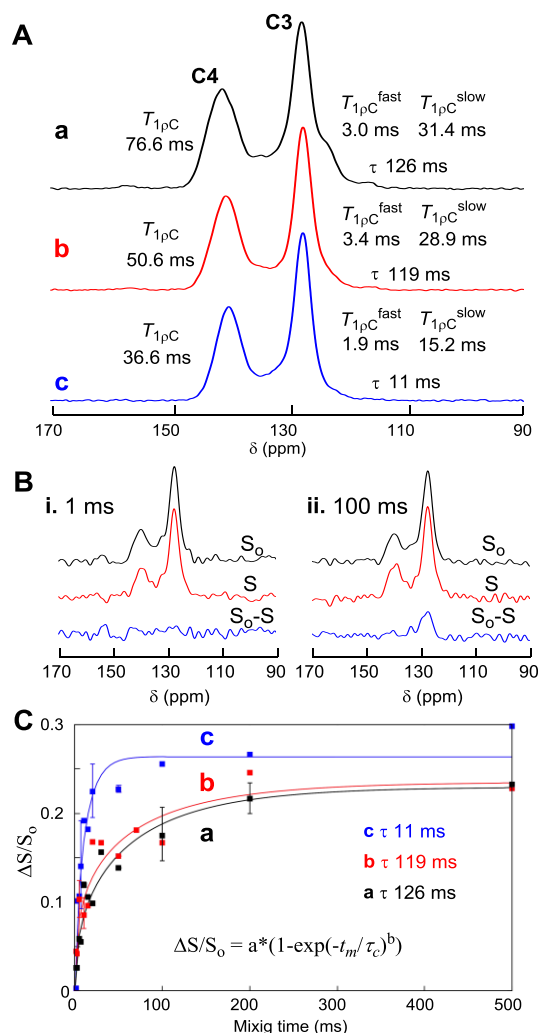

Fig. 3. ^{13}C CPMAS NMR spectra of poly(Bz135-*alt*-Bz14) COF (run 4 in Table S1 in ESI) (a), poly(Bz135-*alt*-BP44') COF (run 3 in Table S2) (b), and poly(Bz135-*alt*-TP44'') COF (run 3 in Table S3-2 in ESI) (c) [A], ^{13}C CODEX spectra of poly(Bz135-*alt*-TP44'') COF with mixing time of 1 ms (i) and 100 ms (ii) including reference spectra (top), CODEX exchange spectra (middle), and pure exchange spectra (bottom) [B], and normalized pure exchange CODEX intensity of the C3 signals as a function of mixing time for poly(Bz135-*alt*-Bz14) COF (a), poly(Bz135-*alt*-BP44') COF (b), and poly(Bz135-*alt*-TP44'') COF (c) [C]. The fit curve in C is a stretched exponential $a*(1-\exp(t_m/\tau_c)^b)$.

More direct motional information was obtained by "Center band Only detection Exchange" (CODEX) NMR experiments.[34] The CODEX experiment detects slow molecular dynamics resulting from changes in the orientation dependent chemical shift frequencies during the mixing time, t_m. The C3 signals exhibited a pure exchange signal at a sufficient mixing time (100 ms) which was not confirmed for the C4 signals (Fig. 3 B). This is a direct evidence of reorientation of phenylene flip, namely

the twisting motion. The correlation time (τ_c), which reflects molecular motion during mixing time, for C3 was estimated from the pure exchange intensity as a function of t_m (Fig. 3C).[34,35] The obtained τ_c for poly(Bz135-*alt*-TP44'') COF (11 ms) was much shorter than for the other two COF's showing similar values (119 ms, 121 ms), indicating that the twisting motion of benzene-1,4-diyl units occurs much smoother in poly(Bz135-*alt*-TP44'') COF than in the other two COF's. It has been reported that rotation of bezene-1,4-diyl units in linear poly(benzene-1,4-diyl-*alt*-ethene-1,2-diyl) occurs in the millisecond time scale (τ_c = 10 ms).[34] The twisting motion in poly(Bz135-*alt*-TP44'') COF may occur at a similar rate.

The observations discussed so far suggest that the rotation around chirality axes was much more smoothly activated by photo excitation in poly(Bz135-*alt*-TP44'') COF than in the other two in which greater steric crowdedness inside the frameworks can hamper such a motion. The density of branching points (core units) thus sensitively affects the freedom of inner rotation in the COF's.

Soluble HBP's were also subjected to CPL irradiation in solution-cast film (Fig. 4). All three HBP's exhibited clear, mirror-image CD spectra upon L- and R-CPL excitation where the chemical structures were found intact by IR spectra (Fig. S11 in ESI), indicating that CPL has introduced preferred-handed twisted conformation. LD spectral measurements also supported that the CD spectra are attributed to material chirality (Figure S26 in ESI).
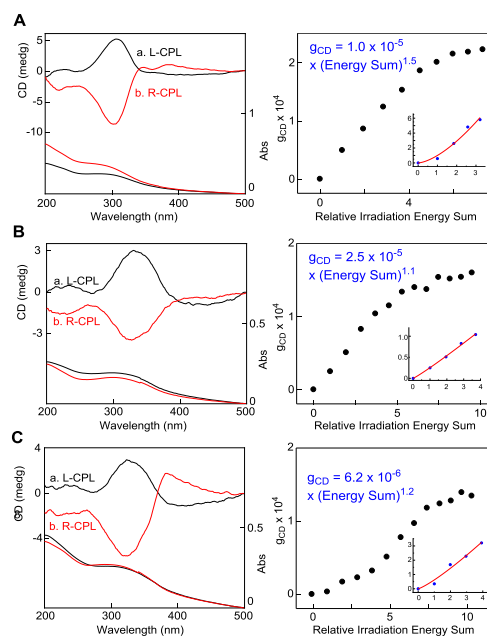

Fig. 4. CD-UV spectra observed on L-CPL (a) and R-CPL (b) irradiation [left] and g_{CD}-vs.-relative irradiation energy sum plots with curve fitting results (inset plots and corresponding equation) [right] of poly(Bz135-*alt*-Bz14) HBP (run 4 in Table S1 in ESI) (A), poly(Bz135-*alt*-BP44') HBP (run 3 in Table S2 in ESI) (B), and poly(Bz135-*alt*-TP44'') HBP (run 3 in Table S3-2 in ESI) (C). Maximum g_{CD} was +2.2 x 10^{-4} at 308 nm (A), +1.6 x 10^{-4} at 331 nm (B), and +1.4 x 10^{-4} at 323 nm (C).

The maximum g_{CD} values were much greater than those expected based only on CPL chirality, and the early-stage data in the g_{CD}-vs.-relative irradiation energy sum plots were well approximated with the power

COMMUNICATION

functions shown in Fig. 4, suggestive of chirality amplification. Chirality induction efficiency was rather similar among the three HBP's while the maximum g_{CD} value and the exponent of power function were slightly greater for poly(Bz135-*alt*-Bz14) HBP than the other two, which may mean that the higher branching density in poly(Bz135-*alt*-Bz14) HBP is advantageous in chirality induction, which was not the case for the COF's.

The sharp contrast in chirality induction between the COF's and the HBP's having the same chemical structures may mean that the COF's have a much more rigid structure based on the extended network than HBP's, and the rotation motion is much more restricted in the COF's. This is supported by the fact that a longer irradiation time was necessary for poly(Bz135-*alt*-TP44'') (up to 45 min) than for the HBP's (up to 10 min) to complete chirality induction.

Also, it is notable that chirality was efficiently induced for the amorphous HBP's because ordered structures enhancing intermolecular interactions have been found crucial in CPL-based chirality induction in both linear polymer and small-molecular systems so far studied.[10-12] Strong enough intra-molecular interactions may be realized even in amorphous structure of HBP's due to the branched architecture.

In conclusion, chirality was successfully induced to poly(Bz135-*alt*-TP44'') COF and the three HBP's, and the distinctive responses to CPL irradiation of the three COF's were rationally understood in terms of the rate of internal rotation rate estimated by the CODEX NMR experiments. For the COF's, chirality induction efficiency was higher when the linker unit was longer as a shorter linker may not allow smooth rotation around chirality axes. Chirality induction to the HBP's was smoother than to the COF's, which may reflect the difference in structural rigidity between the HBP's and the COF's. While there have been various reports of chirality induction using CPL, details of the induced chiral structures and mechanistic features still appear to need further clarification, especially for the examples dealing with polymers in the solid state. The present studies using a series of COF's and HBP's composed of benzene-benzene junctions having systematically altered chemical structures and including a view of conformational dynamics may provide deeper insights into molecular mechanisms of chirality induction by light. Further, the facile preparation of chiral COF's and HBP's using CPL may lead to development of novel optically active, solid-state materials with branching showing various chiral functions.

Conflicts of interest

There are no conflicts to declare.

Notes and references

1   a) E. Yashima, K. Maeda, H. Iida, Y. Furusho, K. Nagai, *Chem. Rev.* **2009**, *109*, 6102–6211; b) E. Yashima, N. Ousaka, D. Taura, K. Shimomura, T. Ikai and K. Maeda, *Chem. Rev.,* **2016**, 116, 13752-13990.

2   a)T. Nakano, Y. Okamoto, *Chem. Rev.* **2001**, *101*, 4013–4038; b) Y. Okamoto. T. Nakano, *Chem. Rev.,* **1994**, *94*, 349-372.

3   A.-M. Caminade, P. Servin, R. Laurent, J.-P. Majoral*, Chem. Soc. Rev.* **2008**, *37*, 56-67.

4   L. Pu, Novel chiral conjugated macromolecules for potential electrical and optical applications. *Macromol. Rapid Commun.* **2000**, *21*, 795-809.

5   D. Seebach, P. B. Rheiner, G. Greiveldinger, T. Butz, H. Sellner, *Top. Curr. Chem.* **1998**, *197*, 125-164.

6   a) X. Han, C. Yuan, B. Hou, L. Liu, H. Li, Y. Liu, Y. Cui, *Chem. Soc. Rev.* **2020**, *49*, 6248-6272; b) X. Guan, F. Chen, Q. Fang, S. Qiu, *Chem. Soc. Rev.* **2020**, *49*, 1357-1384.

7   a) Z. Wang, S. Zhang, Y. Chen, Z. Zhang, S. Ma, Chem. Soc. Rev. **2020**, *49*, 708-735; b) Y. Zhang, X. Jin, X. Ma, Y. Wang, *Anal. Methods* **2021**, *13*, 8-33; c) S. Zhuo, X. Zhang, H. Luo, X. Wang, Y. Ji, *Macromol. Rapid Commun.* **2020**, *41*, 2000404.

8   X. Han, J. Zhang, J. Huang, X. Wu, D. Yuan, Y. Liu, Y. Cui, *Nat. Commun.* **2018**, *9*, 1-10.

9   Y. Wang, T. Sakamoto, T. Nakano, *Chem. Commun.* **2012**, *48*, 1871-1873.

10   Y. Wang, T. Harada, L. Q. Phuong, Y. Kanemitsu, T. Nakano, *Macromolecules* **2018**, *51*, 6865-6877.

11   A. Pietropaolo, Y. Wang, T. Nakano, *Angew. Chem. Int. Ed.* **2015**, *127*, 2726-2730.

12   Y. Wang, A. L. Kanibolotsky, P. J. Skabara, T. Nakano, *Chem. Commun.* **2016**, *52*, 1919-1922.

13   Z. Zhang, T. Harada, A. Pietropaolo, Y. Wang, Y. Wang, X. Hu, X. He, H. Chen, Z. Song, M. Bando, T. Nakano, *Chem. Commun.* **2021**, *57*, 1794-1797.

14   a) A. Imamura, R. Hoffmann, *J. Am. Chem. Soc.* **1968**, *90*, 5379–5385; b) J. Clark, T. Nelson, S. Tretiak, G. Cirmi, G. Lanzani, *Nat. Phys.* **2012**, *8*, 225-231.

15   Z. Zhang, Y. Wang, T. Nakano, *Molecules* **2016**, 21*,* 1541.

16] T. Nakano, *Chem. Rec.* **2014**, *14*, 369-385.

17   A. Pietropaolo, T. Nakano*, J. Am. Chem. Soc.* **2013**, *135*, 5509-5512.

18   A. Pietropaolo, T. Nakano, *Chirality* **2020**, 1-6.

19   L. Nikolova, T. Todorov, M. Ivanov, F. Andruzzi, S. Hvilsted, P. S. Ramanujam, *Opt. Mater. (Amsterdam)* **1997**, *8*, 255–258

20   G. Iftime, F. L. Labarthet, A. Natansohn, P. Rochon, *J. Am. Chem. Soc.* **2000**, *122*, 12646–12650;

21   A. Natansohn, P. Rochon, *Adv. Mater.* **1999**, *11*, 1387–1391.

22   M. Fujiki, K. Yoshida, N. Suzuki, J. Zhang, W. Zhang, X. Zhu, *RSC Adv.* **2013**, *3*, 5213-5219.

23   L. Wang, L. Yin, W. Zhang, X. Zhu, M. Fujiki, *J. Am. Chem. Soc.* **2017**, *139*, 13218-13226.

24   C. He, G. Yang, Y. Kuai, S. Shan, L. Yang, J. Hu, D. Zhang, Q. Zhang, G. Zou, *Nat. Commun.* **2018**, *9*, 1-8.

25   B. L. Feringa, R. A. Delden, *Angew. Chem. Int. Ed.* **1999**, *38*, 3418–3438.

26   T. Kawasaki, M. Sato, S. Ishiguro, T. Saito, Y. Morishita, I. Sato, H. Nishino, Y. Inoue, K. Soai, *J. Am. Chem. Soc.* **2005**, *127*, 3274–3275.

27   R. S. Sprick, B. Bonillo, M. Sachs, R. Clowes, J. R. Durrant, D. J. Adams, A. I. Cooper, *Chem. Commun.* **2016**, *52*, 10008-10011.

28   Catherine M. Aitchison, R. S. Sprick, A. I. Cooper, *J. Mater. Chem. A* **2019**, *7*, 2490-2496.

29   K. V. Rao, S. Mohapatra, C. Kulkarni, T. K. Maji, S. J. George, J. *Mater. Chem.* **2011**, *21*, 12958-12963.

30   A. Pietropaolo, C. Cozza, Z. Zhang, T. Nakano, *Liq. Cryst.* **2018**, *45*, 2048-2053.

31   W. Kuhn, Trans. *Faraday Soc.* **1930**, *26*, 293–308.

32   Y. Inoue, *Chem. Rev.* **1992**, *92*, 741–770.

33   J. Li, G. B. Schuster, K.-S. Cheon, M. M. Green, J. V. Selinger, *J. Am. Chem. Soc.* **2000**, *122*, 2603-2612.

34   E. DeAzevedo, R. Franco, A. Marletta, R. Faria, T. Bonagamba, *J. Chem. Phys.* **2003**, *119*, 2923-2934.

35   W. Hu, T. Bonagamba, K. Schmidt-Rohr*, J. Am. Chem. Soc.* **1999**, *121*, 8411-8412.